The RhoGEF DOCK10 is essential for dendritic spine morphogenesis

Fanny Jaudon, Fabrice Raynaud, Rosine Wehrlé, Jean-Michel Bellanger, Mohamed Doulazmi, Guilan Vodjdani, Stéphane Gasman, Laurent Fagni, Isabelle Dusart, Anne Debant, et al.

The RhoGEF DOCK10 is essential for dendritic spine morphogenesis

Fanny Jaudon[*¶], Fabrice Raynaud[†], Rosine Wehrlé[‡], Jean-Michel Bellanger[*], Mohamed Doulazmi[‡], Guilan Vodjdani[§], Stéphane Gasman[ll], Laurent Fagni[†], Isabelle Dusart[‡], Anne Debant[*#] and Susanne Schmidt[*#]

[*] Centre de Recherche en Biochimie Macromoléculaire, CNRS – UMR 5237, Université de Montpellier, 34293 Montpellier, France
[†] Institute of Functional Genomics, CNRS – UMR 5203, INSERM U661, Université de Montpellier, 34094 Montpellier, France
[‡] Université Pierre et Marie Curie, Université Paris 06, CNRS - UMR 7102, 75005 Paris, France
[§] PROTECT, Neuroprotection du cerveau en développement, UMR1141-INSERM, Université Paris-Diderot, Sorbonne Paris-Cité, 75019 Paris, France
[ll] Institut des Neurosciences Cellulaires et Intégratives, CNRS - UPR 3212, Université de Strasbourg, Centre de Neurochimie, 67084 Strasbourg, France
[¶] Present address: Istituto Italiano di Tecnologia, 16163 Genova, Italy

[#] Co-corresponding authors: susanne.schmidt@crbm.cnrs.fr, anne.debant@crbm.cnrs.fr
Dr Susanne Schmidt/Dr Anne Debant
CRBM- CNRS UMR 5237
1919 Route de Mende
34293 Montpellier Cedex 5, France

Running head: DOCK10 controls dendritic spine formation

Abbreviations

GEF: Guanine nucleotide Exchange Factor
GAP: GTPase Activating Protein
GDP: guanosine diphosphate
GTP: guanosine triphosphate
DOCK: dedicator of cytokinesis
DHR-2: DOCK-homology-region-2
PC: Purkinje Cell
DIV: days *in vitro*

ABSTRACT

By regulating actin cytoskeleton dynamics, Rho GTPases and their activators RhoGEFs are implicated in various aspects of neuronal differentiation, including dendritogenesis and synaptogenesis. Purkinje cells (PCs) of the cerebellum, by developing spectacular dendrites covered

with spines, represent an attractive model system in which to decipher the molecular signalling underlying these processes.

To identify novel regulators of dendritic spine morphogenesis among members of the poorly characterised DOCK family of RhoGEFs, we performed a gene expression profiling of FACS-purified murine PCs, at various stages of their postnatal differentiation. We found a strong increase in the expression of the Cdc42-specific GEF DOCK10. Depleting DOCK10 in organotypic cerebellar cultures resulted in dramatic dendritic spine defects in PCs. Accordingly, in mouse hippocampal neurons, depletion of DOCK10 or expression of a DOCK10 GEF-dead mutant led to a strong decrease in spine density and size. Conversely, overexpression of DOCK10 led to increased spine formation. We show that DOCK10 function in spinogenesis was mediated mainly by Cdc42 and its downstream effectors N-WASP and PAK3, although we found that DOCK10 was also able to activate Rac1. Our global approach thus identified an unprecedented function for DOCK10 as a novel regulator of dendritic spine morphogenesis, via a Cdc42-mediated pathway.

INTRODUCTION

Rho family GTPases are potent determinants of cell shape that regulate actin cytoskeleton and microtubule dynamics, membrane dynamics and vesicular trafficking (Etienne-Manneville and Hall, 2002). They require precise spatio-temporal activation in order to execute their functions. This is in part achieved by their main regulators, the RhoGEFs and the RhoGAPs, which stimulate GDP to GTP exchange and GTP hydrolysis, respectively. RhoGEFs belong to two distinct classes of proteins: the Dbl family and the evolutionary distinct family of DOCK (Dedicator of cytokinesis) proteins (Cote and Vuori, 2007; Schmidt and Hall, 2002). In mammals, the 11 DOCK proteins activate Rac1 or Cdc42 through their catalytic DOCK-homology-region-2 (DHR-2) domain (Cote and Vuori, 2007). Based on sequence similarity, they have been grouped in four subfamilies. The DOCK-A and DOCK-B subfamilies contain Rac-specific GEFs, the DOCK-C subfamily comprises dual-specificity Rac- and Cdc42-GEFs (Pakes et al., 2013), and the DOCK-D subfamily members, also referred to as zizimins (DOCK9/zizimin1, DOCK10/zizimin3 and DOCK11/zizimin2), have been reported to act as Cdc42-specific GEFs (Lin et al., 2006; Nishikimi et al., 2005).

As central to the regulation of cytoskeleton dynamics, Rho GTPase signalling contributes to various cellular processes, including different steps of neuronal differentiation, such as the morphogenesis of dendrites and spines (Govek et al., 2005). Development and maturation of dendrites are complex, multistep processes that must be finely tuned. This has been well described in the Purkinje cells (PCs) of the cerebellum, which have a very elaborate dendritic tree and therefore

represent an attractive model system to study this process (Sotelo and Dusart, 2009; Tanaka, 2009; Urbanska et al., 2008). The development of PC dendrites follows sequential stages to finally reach, at the end of the third postnatal week in mice, a mature dendritic tree covered with spines. Dendritic spines are small protrusions that constitute the sites of synaptic contacts, leading to the establishment of neuronal circuits (Yuste and Bonhoeffer, 2004). They are highly dynamic actin-rich structures, which undergo continuous remodelling upon sensory and emotional stimuli, such as those arising during learning and memory. Their dynamic assembly is therefore essential for normal brain function. In hippocampal neurons, the GTPases Rac1 and Cdc42 promote formation and maintenance of dendritic spines, whereas RhoA induces their retraction and loss (Tada and Sheng, 2006). Signalling from these GTPases to the actin cytoskeleton is then mediated by specific downstream effectors, such as the neural Wiskott-Aldrich Syndrom protein N-WASP, PAK family kinases, ROCK or mDia (Kasri and van Aelst, 2008; Newey et al., 2005). The physiological importance of this signalling in dendritic spine morphogenesis is further highlighted by the fact that mutations in several genes of Rho pathway components, like the GAP Oligophrenin-1, the GEF α-PIX and the kinase PAK3, are associated with X-linked mental retardation, characterised by an immature morphology of spines (Govek et al., 2005; Newey et al., 2005).

However a clear picture of the RhoGEFs activating Rho family GTPases during spinogenesis is still lacking. In this study, we sought for novel regulators of dendritogenesis and/or spinogenesis among members of the poorly characterised DOCK family of RhoGEFs, *via* a gene expression profiling of FACS-purified PCs. We identified the RhoGEF DOCK10 as being essential for dendritic spine morphogenesis both in PCs and in hippocampal neurons, via a Cdc42-mediated pathway.

RESULTS

Gene expression profiling during postnatal Purkinje neuron development

In order to identify novel RhoGEFs involved in dendritic tree morphogenesis, we undertook a gene expression profiling of all DOCK family RhoGEFs in Purkinje cells. Since these neurons represent only 2-3% of the whole cerebellum, we took advantage of a mouse strain carrying the green fluorescent protein (GFP) under the Purkinje-specific promoter Pcp2, to purify the PCs by fluorescence-activated cell sorting (FACS) (Tomomura et al., 2001). Neurons were isolated from cerebella of postnatal day P3-, P7-, P15- and P20-old Pcp2-GFP mice, corresponding to the timeframe of development of the Purkinje cell dendritic tree. Purity of the Purkinje cell samples was assessed both by visual counting of the Calbindin-positive cells (Calbindin is a Purkinje cell specific marker) before and after sorting (Figure 1A-C) and by real-time quantitative PCR (RT-qPCR) of marker genes specific for the Purkinje cells (Calbindin) and for the other main cerebellar cell types, i.e. granule cells

(NeuroD1), astrocytes (GFAP) and interneurons (Tcfap2a) (Figure 1D). After sorting, Purkinje cells represented around 78% of the cell population.

We then performed RT-qPCR on mRNAs isolated from these cells and analysed the expression pattern of all 11 members of the mammalian DOCK family of RhoGEFs in the course of development (Figure 1E, see Table S1 for primer sequences). The mRNAs of DOCK180/DOCK1, DOCK2, DOCK3 and DOCK8 could not be detected, due to too low expression levels. DOCK4, DOCK5, DOCK6 and DOCK7 were expressed, but their mRNA levels did not vary significantly across the 4 developmental stages we analysed, except for DOCK4 and DOCK6 whose expression dropped at P20. In contrast, the three DOCK-D subfamily members, i.e. DOCK9, DOCK10 and DOCK11, showed a significant increase in their mRNA expression levels, reaching a peak at P15 (DOCK11) or P20 (DOCK9 and DOCK10) (Figure 1E). We identified DOCK10 as a promising candidate since its robust increase in expression occurred precisely during the timeframe of Purkinje cell spinogenesis during the second and third postnatal week, and since no neuronal function had been ascribed to this protein so far.

DOCK10 is expressed in Purkinje cells during postnatal development

To confirm the RT-qPCR data and address the expression of the DOCK10 protein in the postnatal cerebellum, we analysed the expression pattern of DOCK10 in post-natal mouse brain slices, by immunohistochemistry (IHC) using a DOCK10-specific antibody (Figure 2). In whole sections of the cerebellum (P15), the DOCK10 protein was detected in the monolayer of Purkinje cells (PCL), nicely overlapping with the Purkinje-specific Calbindin staining (Figure 2A). Higher magnification images showed that at P7, and more strikingly at P15 and later stages, DOCK10 was detected in the soma and the dendritic tree of PCs, although it was only weakly detectable in the latter (Figure 2A inset and Figure 2B). At P7, DOCK10 immunostaining could also be seen in the external and internal granule cell layer (EGL and IGL), but at P15 and P21, IGL staining disappeared and DOCK10 localisation seemed to be restricted to the Purkinje cell layer (Figure 2B).

Altogether, these data show that, at early postnatal stages, DOCK10 is expressed broadly in the cerebellum and that from P15 on, its expression becomes restricted to the Purkinje cells.

Depletion of DOCK10 in Purkinje cells leads to dendritic spine defects

Given the expression of DOCK10 in differentiating Purkinje neurons, we investigated the function of DOCK10 in these cells, by analysing the effect of knocking down its expression. To do so, we designed and validated two different shRNAs targeting DOCK10 (shA and shB), or a control shRNA (shCtrl) (see Materials and Methods). Both shRNAs targeting DOCK10 efficiently knocked down endogenous DOCK10 expression (Figure S1A) and were ineffective on the closely related DOCK9 and DOCK11 RhoGEFs (Figure S1B). We then transduced mouse cerebellar organotypic cultures at P0 with

lentiviral vectors expressing these shRNAs and carrying also the GFP as a transduction marker. In these organotypic slices, the dendritic development of Purkinje cells is almost similar to that observed *in vivo*, although in a slightly delayed manner (Boukhtouche et al., 2006; Poulain et al., 2008). Slices were grown until 14 DIV and, after fixation, PC morphology was analysed by immunofluorescence staining with a Calbindin antibody. On the same slice, transduced (Calbindin+/GFP+) versus non-transduced (Calbindin+/GFP-) Purkinje cells could be visualized (Figure 3A), allowing for an accurate comparison of the cell morphology whatever the transduced state. A blinded analysis was then conducted in order to analyse whether the knock down of DOCK10 affected the general dendritic morphology of Purkinje cells (see Materials and Methods). To do so, all the Purkinje cells were distributed into three groups, depending on their dendritic morphology observed by Calbindin immunostaining (Figure 3B): PCs with an atrophic morphology (the longest dendrite being smaller than the cell body diameter), PCs with a stellate morphology (harbouring more than six perisomatic processes) and PCs with an elaborate dendritic tree.

No statistically significant difference could be detected in the distribution within these three groups of PCs, whether transduced or not with shA or shB DOCK10, or shCtrl lentivectors (Figure 3C), suggesting that knock-down of DOCK10 expression does not have a major effect on overall Purkinje cell dendritic development.

However, a more careful analysis of the elaborate Purkinje cells revealed two types of cells: the ones presenting at least one part of the dendritic tree covered with spines (Figure 3D, panel D1) and the ones with a dendritic tree totally devoid of spines (Figure 3D, panels D2 and D3). Nearly all the non-transduced PCs and the PCs transduced with ShCtrl presented an elaborate dendritic tree with spines (Figure 3D and E). In contrast, 53% and 23% of Purkinje cells transduced with shA-DOCK10 and shB-DOCK10, respectively, presented a dendritic tree completely devoid of spines (Figure 3D and E). This defect was observed with both shRNAs, albeit to a lesser extent with Lv-ShB, excluding an off-target effect.

To determine whether depletion of DOCK10 acted only on the formation of spines or whether the observed phenotype was an indirect consequence of defective dendritic tree morphogenesis, a Sholl analysis was performed on these elaborate Purkinje cells to measure the complexity and height of the dendritic tree (see Materials and Methods) (Figure 3F). The general distribution of the Sholl index was the same, whether the cells were transduced with shCtrl or shA- or shB-DOCK10. The large majority of the branching points were observed between 20µm and 40µm from the soma (Figure 3F). Although the Sholl index at 30µm from the soma varied between the different Lv transduced conditions (from 4.6 to 7.7), these differences were not correlated with the presence or absence of spines. Therefore, this analysis revealed no significant effect of any shRNA on

the complexity or height of the dendritic tree of elaborate PCs, showing a direct role for DOCK10 in dendritic spine morphogenesis.

DOCK10 is required for the formation of dendritic spines in hippocampal neurons

In order to better characterise the function of DOCK10 in dendritic spine morphogenesis, we turned to primary cultures of hippocampal neurons, which are a classical model to study spine morphogenesis and which are more tractable to culture and transfection than Purkinje cells. We first verified that DOCK10 was expressed in the postnatal mouse hippocampus. Indeed, Western blot analysis performed on lysates of different P26 mouse brain areas and on lysates of cultured hippocampal neurons (at 18 DIV) revealed the expression of DOCK10 in the hippocampus, but also in the olfactory bulb and the cortex (Figure 4A). The hippocampal expression of DOCK10 was also confirmed by IHC analysis on P15 mouse brain sections, using a DOCK10 antibody (Figure 4C). This revealed that DOCK10 was present in the pyramidal cells of the CA1 and CA3 regions, as well as in the adjacent subiculum and the dentate gyrus.

We then studied the specific sub-cellular localisation of endogenous DOCK10 by performing fractionation experiments on a sucrose gradient. This showed that DOCK10 was present in the synaptosomal fraction, where it fractionated together with the post-synaptic density protein PSD-95 (Figure 4B), indicating a synaptic localisation for DOCK10. Both proteins were also detected in the membrane fraction. Interestingly, Cdc42, the target GTPase of DOCK10, was also detected in these two fractions (Figure 4B). We further confirmed the synaptosomal localisation of DOCK10 by immunofluorescence studies, by transfecting flag-DOCK10 into cultured hippocampal neurons. Figure 4D shows that DOCK10 was localised in the dendritic shaft and most strikingly in the dendritic spines in hippocampal neurons, which is compatible with a function of DOCK10 in dendritic spine morphogenesis. In addition, DOCK10 immunostaining in the spines localised adjacent to the pre-synaptic protein Bassoon (Figure 4E). Combined, these data show that DOCK10 is present in the post-synaptic density.

We next analysed the consequences of DOCK10 depletion on spine formation in hippocampal neurons, by transfecting them at 8 DIV (before the initial appearance of the spines) and fixing them three days later. ShRNA-mediated depletion of DOCK10 led to a dramatic decrease in the number of spines along the dendritic shaft (Figure 5, A and B). This defect was accompanied by a decrease in spine head size in the remaining spines (Figure 5C). In addition, the post-synaptic density protein Homer-1 was hardly detected by immunofluorescence in the remaining protrusions of DOCK10-depleted neurons, as compared to control neurons, confirming that spines devoid of DOCK10 are not properly formed (Figure 5, D and E). To confirm the requirement of DOCK10 for

spine formation, we performed rescue experiments by re-introducing a shRNA-resistant DOCK10 construct into DOCK10-depleted hippocampal neurons. This construct was designed such as to be resistant only to shA DOCK10 and not to shB, as demonstrated in Figure S2A (see Materials and Methods). As shown in Figure 5, F and G, wt DOCK10^{shR} was able to rescue the decrease in both spine number and spine head size induced by shA-mediated DOCK10 depletion, demonstrating its requirement for spine morphogenesis.

To determine whether the dependency on DOCK10 for spine formation required its GEF activity, we created a catalytically inactive mutant, based on a similar mutant in DOCK9 (Yang et al., 2009). In this mutant, the catalytic DHR2 domain harbours a point mutation abolishing its GEF activity, as assessed by *in vitro* GEF assays on Cdc42 (Figure S2B). Interestingly, this GEF-dead mutant DOCK10 (DOCK10^{shR} GD) was unable to rescue the spine defects induced by DOCK10-depletion (Figure 5, F and G), indicating that the GEF activity of DOCK10 is indeed required for proper morphogenesis of dendritic spines.

DOCK10 is a GEF for Rac1 and for Cdc42 *in vitro* and in cells

Both Cdc42 and Rac1 GTPases are involved in different aspects of spine development, promoting growth and/or stability of dendritic spines (Tada and Sheng, 2006). This prompted us to ask whether Cdc42 and Rac1 could be targets of DOCK10 in this process. Intriguingly, all DOCK-D subfamily GEFs, including DOCK10, have been reported as Cdc42-specific GEFs. In non-neuronal cell lines, DOCK10 has been described as a GEF specific for Cdc42, both by GTPase binding assays and by active GTPase pull-down assays (Gadea et al., 2008; Nishikimi et al., 2005). However, the exchange activity of DOCK10 on Cdc42 has never been formally shown *in vitro*, in contrast to that of DOCK9 and DOCK11 (Cote and Vuori, 2002; Lin et al., 2006).

To clarify this issue, we performed *in vitro* GEF assays on recombinant Cdc42, Rac1 and RhoA (Figure 6, A and B, Figure S3A). The catalytic DHR2 domains of DOCK9, DOCK10 and DOCK11 (as defined by (Cote and Vuori, 2006)), were produced as recombinant proteins in bacteria and used in a mant-GTP fluorescence kinetics assay (Bouquier et al., 2009). In this assay, the DHR2 domains of DOCK9, DOCK10 and DOCK11 promoted GDP/GTP exchange on Cdc42, and not on RhoA, as expected from previous data (Figure 6A and S3A) (Cote and Vuori, 2002; Lin et al., 2006). Surprisingly, DOCK10 DHR2 was also able to activate directly Rac1, in contrast to the other two GEFs, establishing DOCK10 as the sole dual-specificity RhoGEF of the DOCK-D subfamily (Figure 6B).

To confirm these *in vitro* data in intact cells, Cdc42-GTP, Rac1-GTP and RhoA-GTP pull-down experiments were performed, using the CRIB-domain (Cdc42/Rac1 Interactive Binding) of WASP and PAK1, and the RBD-domain (RhoA-binding domain) of Rhotekin, respectively (Figures 6, C, D, E and S3B). Cdc42-GTP, but not RhoA-GTP, was efficiently pulled-down from HEK293T cells expressing all

three full length DOCK proteins (Figure 6C and S3B). Rac1-GTP, in contrast, was only and very efficiently pulled-down from cells expressing full length DOCK10 (Figure 6D), thus confirming the *in vitro* data. To rule out the possibility that this activation of Rac1 by DOCK10 in cells was indirect, we made use of the GEF-dead point mutant of DOCK10 (DOCK10 GD) described above. When expressed in cells, this mutant was unable to elicit the robust activation of Rac1 observed with wild-type DOCK10 (Figure 6E). Thus, these data show that DOCK10 is a *bona fide* GEF for Rac1.

Taken together, our results reveal DOCK10 as a dual-specific GEF, activating both Cdc42 and Rac1, *in vitro* and in cells, whereas the other subfamily members DOCK9 and DOCK11 are strictly specific for Cdc42.

Cdc42 GEF activity is required for DOCK10-mediated spine formation

Next we asked which of these GTPases would be the target(s) of DOCK10 for its function on spine morphogenesis. To do so, we transfected cultured hippocampal neurons at 8 DIV with DOCK10 and with well-established shRNAs targeting Cdc42 or Rac1 (Momboisse et al., 2009) or with a control shRNA (shCtrl). As expected, expression of shRNAs targeting Rac1 or Cdc42 alone significantly decreased spine number along the dendrites, as compared to shCtrl (Figure 7, A and B). Overexpression of DOCK10 (with shCtrl) increased moderately but significantly spine density (Figure 7, A and B), confirming its positive effect on spine formation. In contrast, co-expression of shCdc42 with DOCK10 markedly suppressed this effect, and this was not the case with shRac1. Taken together, these data suggest that DOCK10 signals essentially through Cdc42 for spine formation.

To confirm that DOCK10 acted through Cdc42 for its effect on spine formation, we tested whether dominant negative forms of Cdc42-specific effectors, such as the neural Wiskott-Aldrich syndrome protein (N-WASP) and PAK3, were able to block DOCK10-mediated spinogenesis. N-WASP has been shown to mediate a direct connection between Cdc42 and the Arp2/3 complex for actin polymerization (Rohatgi et al., 1999). Group 1 PAK kinases are effectors of both Cdc42 and Rac1, but PAK3 has been shown to bind preferentially Cdc42 (Kreis et al., 2007). Both N-WASP and PAK3 are critical regulators of spine morphogenesis (Kreis et al., 2007; Wegner et al., 2008). As shown previously, expression of N-WASPΔWA, a construct encoding N-WASP deleted of its C-terminal WA domain and thus unable to bind the Arp2/3 complex and G-actin (Figure S4; (Wegner et al., 2008)), or expression of this domain alone (N-WASP WA), affected the number of spines in cultured hippocampal neurons (Figure 7C). Expression of a kinase-dead form of PAK3 (PAK3 KD, Figure S4) also affected spine number (Figure 7C). Strikingly, co-expression of DOCK10 with either N-WASPΔWA or N-WASP WA or PAK3 KD impaired DOCK10's effect on spine formation (Figure 7C).

To further demonstrate that DOCK10 activated Cdc42 to promote the formation of spines, we examined whether the poor spine morphology induced by DOCK10 depletion could be rescued by

co-expressing wt N-WASP or PAK3. This showed that expression of either N-WASP or PAK3 nicely rescued the defect in spine formation due to DOCK10 depletion (Figure 7D), to a similar extent as did re-introduction of DOCK10^{shR} (Figure 5F).

All combined, these data argue for N-WASP and PAK3 mediated pathways downstream of DOCK10/Cdc42 functioning in spine morphogenesis.

DISCUSSION

Cognitive functions, such as learning and memory, rely on proper morphogenesis of dendritic spines and plasticity of brain synapses. Their establishment is initiated by small actin-rich protrusions called dendritic filopodia, which are long, thin protrusions abundantly present in developing neurons, and which can then be transformed morphologically and functionally into spines. In the adult, dendritic spines also undergo continuous remodelling of their shape and number, upon sensory and emotional stimuli, which requires reorganisation of their actin cytoskeleton. In this study, we show that the atypical RhoGEF DOCK10 is a novel regulator of the formation of dendritic spines in developing neurons. This work is the first report of a neuronal function of DOCK10, whose activity has been implicated so far only in amoeboid invasion of melanoma cells (Gadea et al., 2008). DOCK10 is expressed in post-natal developing Purkinje neurons, when the dendritic tree and spines are being formed. Consistently, we show that DOCK10 is essential for the formation of the spines, not only in Purkinje cells, but also in cultured hippocampal neurons, suggesting that DOCK10 may function as a general regulator of spine morphogenesis. In support of this, a recent human genetics study showed that deletion of the *DOCK10* gene, together with the presence of a hemizygous missense variant, is associated with autism spectrum disorders (ASDs) (Nava et al., 2013). ASDs are neuropsychiatric diseases that are often characterized by developmental alterations of spines and loss of synaptic plasticity, and many of the genes that are mutated in ASDs are crucial components of the activity-dependent signalling networks that regulate synapse development and plasticity.

By controlling actin cytoskeleton dynamics, Rac1 and Cdc42 signalling pathways have been shown to play a key role in regulating spine formation and/or stability in hippocampal neurons (Vadodaria et al., 2013). Cdc42 is important for neural stem/progenitor cell proliferation, initial dendritic development and spine maturation, while Rac1 regulates late steps of dendritic growth and spine maturation. These pathways are regulated by several different signalling complexes including protein kinases and RhoGEFs. Indeed, RhoGEFs belonging to the Dbl-family, mostly the Rac1-specific GEFs like Kalirin-7, βPIX and Tiam-1, but also the Cdc42-specific Intersectin, have been reported for some time now to be localised to dendritic spines and to be implicated in spine development and synaptic plasticity in hippocampal neurons (for review see (Kiraly et al., 2010; Tolias et al., 2011)).

Only very recently have DOCK-family RhoGEFs, i.e. the two Rac1-specific DOCK180 and DOCK4, emerged as being also required in the process of spine formation (Kim et al., 2011; Kuramoto et al., 2009; Ueda et al., 2013). In the case of DOCK180, a signalling module composed of RhoG/ELMO1/DOCK180 has been shown to regulate spine morphogenesis in hippocampal neurons by activating Rac1 (Kim et al., 2011). DOCK4, which also interacts with ELMO2 to activate Rac1, requires an association with Cortactin to mediate its effect on hippocampal spine formation (Ueda et al., 2013). Intriguingly, we detected no increase in mRNA expression of either of these two GEFs during Purkinje cell dendritic development. Among the DOCK-D subfamily members, only DOCK9 has been shown to be involved in dendritic formation, but no function in spine morphogenesis has been described (Kuramoto et al., 2009). Our findings now add the RhoGEF DOCK10 to the picture, localising to dendritic spines and acting as an essential regulator of spine morphogenesis both in the hippocampus and the cerebellum. Our work shows that DOCK10 regulates spine formation by promoting actin polymerisation *via* Cdc42 activation, although we cannot totally exclude a function of Rac1 in this process, like during spine maintenance for instance. Our data suggest that N-WASP and PAK3 both mediate spine formation downstream of DOCK10-Cdc42. Indeed, N-WASP truncation mutants and PAK3 KD mutant block DOCK10's effect on spine formation and both wt N-WASP and PAK3 rescue the defects induced by DOCK10 depletion. By activating the actin nucleation complex Arp2/3, N-WASP thus provides a direct connection between DOCK10/Cdc42 and actin cytoskeleton remodelling in spines. This is in agreement with previous findings in melanoma cells, showing that N-WASP and DOCK10 were found in the same complex during amoeboid motility (Gadea et al., 2008). PAK3 controls actin cytoskeleton remodelling through LIM kinase-mediated cofilin phosphorylation (Ba et al., 2013), thus linking the DOCK10/Cdc42 module to actin cytoskeleton remodelling in spines. Together, these data argue for N-WASP- and PAK3-mediated pathways downstream of DOCK10/Cdcd42, functioning in spine morphogenesis.

DOCK family RhoGEFs usually exhibit a high specificity towards either Rac1 or Cdc42, as compared to the RhoGEFs of the Dbl family that can often activate several GTPases. Interestingly, our data demonstrate that DOCK10 differs from the other two members of the DOCK-D subfamily of GEFs, as it acts as a dual-specificity GEF activating both Rac1 and Cdc42 *in vitro* and in cells. So far, all three members of the DOCK-D subfamily of GEFs, DOCK9/10/11, had been reported to be specific for Cdc42 (Lin et al., 2006; Nishikimi et al., 2005). DOCK10 therefore emerges as a peculiar GEF of this subfamily. The molecular mechanisms of GDP-GTP exchange and the nature of the determinants responsible for the specificity of DOCK proteins towards their GTPase targets have been proposed following the recent elucidation of the structure of the DHR-2 domains of DOCK9 and DOCK2 in complex with Cdc42 and Rac1, respectively (Kulkarni et al., 2011; Yang et al., 2009). The selectivity of the DHR-2 domain is conferred mainly by two regions in the GTPase, a Phe or Trp residue in position

56 and an Ala or Lys residue at position 27 for Cdc42 and Rac1, respectively. However, the relative divergence between DHR-2 domains precludes an easy identification of the amino acids of the DHR-2 domain participating in the GTPase specificity. For example, Leu 1941 in the Cdc42-specific DOCK9 is a Met in the Rac1-GEF DOCK2 and these amino-acids contact Phe56 or Trp56 of the Cdc42 and Rac1 GTPases, respectively. However, these residues are not sufficient to account by themselves for the GTPase selectivity, since DOCK10, which activates both Cdc42 and Rac1, harbours a Leu at this position, like DOCK9. This suggests that multiple, crucial amino-acids are required for the GTPase selectivity of DHR-2 domains. Further studies will be required to define these residues.

How DOCK10 activity itself is regulated remains an open question as well. On a molecular level, most structure-function analyses have been conducted so far on the DOCK-A and -B subfamilies, whose regulation involves their N-terminal SH3 domain (Lu et al., 2005). Like the other DOCK-D subfamily members, DOCK10 harbours a PH domain, instead of an SH3 domain, within its N-terminus. PH domains have been shown to be important for modulating GEF activity and localisation of Dbl-family GEFs via interaction with proteins or phosphoinositides. The precise function of this domain in DOCK-D family GEFs still remains to be determined. In addition, the DHR-1 domain may target DOCK10 to the plasma membrane, as it has been described for the prototypic DOCK180 GEF (Cote et al., 2005). This could represent a means to specifically localise DOCK10 at the postsynaptic density under the surface membrane of spine heads, for example. Consistently, we have detected DOCK10 in the membrane and synaptosomal fractions of brain extracts. In addition, we have observed an increased expression of DOCK10 protein during PC development, which could then account for an increased activity of the protein in the spines. Upstream signalling pathways that would impinge on and activate DOCK10 also remain still unknown, as is the case for the other DOCK family RhoGEFs, and their identification is essential to gain insights into the overall neuronal spectrum of activity and regulation of DOCK10. Possible candidate upstream regulators of DOCK10 that could be tested include neurotransmitter receptors such as NMDA or AMPA receptors, or the EphB receptor, which have been shown for example to translocate the Dbl-RhoGEFs Tiam1 and Kalirin-7 to the postsynaptic region and to enhance their GEF activity (Penzes et al., 2003; Tolias et al., 2005; Tolias et al., 2007).

In conclusion, the atypical RhoGEF DOCK10 emerges as a novel, crucial regulator of dendritic spine morphogenesis in the hippocampus and the cerebellum, and, given its strong expression in several other brain areas, it could potentially play additional roles in neuronal development which still remain to be explored.

MATERIALS AND METHODS

DNA constructs

IMAGE clones for mouse DOCK10 and DOCK9 were obtained from Source Bioscience. DOCK11 plasmid was a kind gift of Dr Mitsuo Maruyama (Aichi, Japan). The cDNAs were subcloned into pEGFP or pmCherry vectors by PCR amplification, flanking the construct with restriction enzymes appropriate for subcloning. The DHR-2 domains of DOCK9/10/11 were subcloned into the pEGFP or the pGEX vectors by PCR amplification of the appropriate fragment of the three clones. The GEF-dead DOCK10 mutant was generated by introducing a point mutation at V2055A in the wild-type form of DOCK10, using the Quick Change site-directed mutagenesis kit (Stratagene), according to the manufacturer's instructions. The shRNA-resistant mutant of DOCK10 was created by introducing 4 point mutations in the DNA sequence of DOCK10 targeted by shA, to render it unrecognisable by the shA shRNA. Details on cloning procedures and on primer sequences can be obtained upon request. RFP-PAK3 and RFP-PAK3 K297L (kinase dead mutant) were kind gifts of Jean-Vianney Barnier (CNRS, UMR 8145, Paris). mCherry N-WASP, N-WASP ΔWA and N-WASP WA construct were kindly provided by Nathalie Morin (CRBM, Montpellier) and Michael Way (Cancer Research UK, London Research Institute).

Antibodies

The following primary antibodies were purchased: anti-GFP polyclonal antibody (Cliniscience); anti-DOCK10 polyclonal antibody (Bethyl Lab.); anti-α-Tubulin monoclonal antibody (Sigma); anti-Rac1 and anti-Cdc42 monoclonal antibodies (BD Biosciences); anti-Calbindin monoclonal antibody (Swant); anti-PSD95 monoclonal antibody (clone 7E3, Santa Cruz); anti-Bassoon monoclonal antibody (Enzo Life Sciences); anti-Homer-1 monoclonal antibody (Synaptic Systems); anti-flag M2 monoclonal antibody (Sigma).

The following secondary antibodies were used: Alexa Fluor 350-, 488-, 546- and 594-conjugated anti-rabbit/mouse antibodies (Invitrogen) for immunofluorescence studies, and anti-mouse or anti-rabbit IgG coupled to Horseradish Peroxidase for Western immunoblotting (GE Healthcare). Hoechst was used to detect nuclei.

Animals

Male and female Pcp2-GFP or wild type C57BL/6 mice (Jackson Laboratories) and Swiss mice (Janvier,

France), used for organotypic cultures and for primary cultures of hippocampal neurons, were housed at the animal house facility of the IGMM (Institut de Génétique Moléculaire de Montpellier) or of IFR83 (Paris). Animals had *ad libitum* access to food and water with 12 hour light-dark cycle.

Purkinje cell sorting

Purkinje cells were isolated from Pcp2-GFP mice as described (Tomomura et al., 2001). Briefly, cerebella were removed from mice at the indicated ages. Cubes (0.5-mm^3) of cerebella were digested for 10 min at 37°C with 0.025% Trypsin (type I; Sigma-Aldrich, Saint Louis, MO) in dissociation solution consisting of Ca^{2+}-free Hanks' balanced salt solution (HBSS) containing 3 mg/ml BSA, 15 mM Hepes, 1.5 mM $MgSO_4$, and 3 mg/ml glucose (pH 7.4). The enzymatic reaction was stopped by the addition of dissociation solution containing 0.25 mg/ml soybean Trypsin inhibitor, 40 µg/ml DNase I, 50 µM APV, 20 µM DNQX and 0.1 µM TTX (all from Sigma-Aldrich). Tissues were triturated mildly by sequential passage through wide-bore and fine-tipped pipettes. Cells were filtered through a 40 µm nylon mesh, and were resuspended in Ca^{2+}- and Mg^{2+}-free dissociation solution at a final concentration of 5.10^6 cells/ml. To label dead cells, PI (Propidium iodide; Sigma-Aldrich) was added at a final concentration of 2 µg/ml. Cell sorting was performed on a FACsAria machine. The sorting decision was based on the measurements of FSC, PI fluorescence and GFP fluorescence.

RNA preparation and real time quantitative RT-PCR of purified Purkinje cells

Total RNA was extracted with Trizol reagent (Invitrogen) from approximately 3.10^4 purified Purkinje cells at the indicated stages. The corresponding cDNAs were prepared by reverse transcription of 100 ng RNA using SuperScript III First-Strand Synthesis System (Invitrogen) with an oligo-dT primer according to the manufacturer's instructions. The resulting cDNAs were used as a template for real-time quantitative PCR using a Light Cycler 480 thermocycler (384 plates, Roche Diagnostics) with a home-made SYBR Green QPCR master mix (Lutfalla and Uze, 2006). Thermal cycling parameters were 2 min at 95°C, followed by 45 cycles of 95°C for 10 s, 64°C for 15 s and 72°C for 25 s. The relative quantification in gene expression was determined using the $\Delta\Delta$Ct method. To normalize expression data, primers for ten commonly used housekeeping genes were used and the normalization factor was determined using the geNorm software, as described in (Vandesompele et al., 2002). This led to the selection of the following internal control genes in our assays: GAPDH, β-Actin and HPRT1. Sequences of the primers used are listed in Table S1.

Immunohistochemistry

For immunohistochemistry, mice were perfused trans-cardiacally with 4% paraformaldehyde in 0.12M phosphate buffer, pH 7.4. Brains were removed, post fixed overnight in 4% PFA, cryoprotected in 20% then 30% sucrose, embedded in OCT, frozen in isopentane (-55°C) and stored at -80°C. Sagittal sections (10 µm) were cut with a cryostat and stored at -20°C prior to immunostaining. Sections were rehydrated in PBS for 5 min, then fixed and permeabilized with 70%

methanol - 30% acetone for 15 min at -20°C. After washes in PBS, slices were blocked for 30 min in PBS containing 1% BSA and incubated with primary antibodies diluted in PBS 1% BSA for 2h at room temperature. After washes in PBS containing 0.25% Tween-20, slices were incubated with secondary antibodies diluted in PBS 1% BSA for 45 min at room temperature. After washes, sections were mounted with Mowiol.

Recombinant lentiviral vectors: construction and production

Plasmid constructions. To inhibit DOCK10 expression, two short hairpin RNAs directed against DOCK10 mRNA were selected for their inhibitory efficiency. Their corresponding DNA sequences are:

ShA: 5′-GATCCCCGCACAGAGCTGAATCCTATTTCAAGAGAATAGGATTCAGCTCTGTGCTTTTTA-3′;

ShB: 5′-GATCCCCCAAGGCACGGAATATAACTTTCAAGAGAAGTTATATTCCGTGCCTTGTTTTTA-3′. These two sequences were inserted as a DNA cassette under the control of the polymerase III-dependent H1 promoter, into the pFlap-PGK-EGFP-ΔU3 vector (Santamaria et al., 2009), generating the pFlap-H1-shRNA-PGK- EGFP-ΔU3 series of vectors hereafter named shA-DOCK10 and shB-DOCK10. The scrambled control shRNA vector, shScr, corresponding to a random shA-DOCK10 sequence

(5'-GATCCCCGGCAAATTAGCCACGTACTTTCAAGAGAAGTACGTGGCTAATTTCGGTTTTTA-3') or a non-relevant control shRNA vector, Lv-shRd, consisting of a random sequence (5'-GATCCCCTCGTCATAGCGTGCATAGGTTCAAGAGACCTATGCACGCTATGACGATTTTTGGAAA-3') were used as control, and collectively referred to as shCtrl throughout the study.

Lentiviral production. Stocks of viral particles were prepared as described previously (Zennou et al., 2001) by transient co-transfection of HEK 293T cells with the p8.91 encapsidation plasmid (Zufferey et al., 1997), the pHCMV-G (Vesicular Stomatitis Virus pseudotype) envelope plasmid and the pFlap vectors described above. Briefly, the supernatants were collected 48 hours after transfection, treated with DNAse I (Roche Diagnostics) and filtered before ultracentrifugation. Viral pellets were then resuspended in PBS, aliquoted and stored at -80°C until use. The amount of p24 capsid protein was determined by the HIV-1 p24 ELISA antigen assay (Beckman Coulter, Fullerton, CA). Viruses from different productions averaged 300 ng/µl of p24 antigen and 3.10^8 TU/ml (Transducing units).

Organotypic slice culture, lentiviral–mediated transduction and immunostaining

Cerebellar organotypic cultures were set up from newborn (P0) mice as previously described (Lebrun et al., 2013). Mice were decapitated and their brains were dissected out in cold Gey's balanced salt solution (Invitrogen) supplemented with 5 mg/ml glucose. Cerebellar parasagittal slices (350 µm thick) were cut on a McIlwain tissue chopper and transferred onto 30 mm diameter Millipore culture inserts with 0.4 µm pores (Millicell, Millipore). Slices were maintained in culture in six-well plates

containing 1 ml of nutrient medium per well, at 37°C, under a humidified atmosphere containing 5% CO_2. The nutrient medium consisted of basal medium with Earle's salts (BME, Invitrogen) containing 1 mM L-glutamine, 5 mg/ml glucose, 0.5 mg/ml BSA (SIGMA A-4503) and supplements including 5 µg/ml insulin, 5 µg/ml transferrin and 5 µg/ml sodium selenite (SIGMA I-1884). Lentiviral vectors (between 0.5 to 2µl per slice, depending on the lentiviral production) were applied 2-4 hours after culture processing of P0 slices. The medium was replaced every 2–3 days.

Slices were fixed with 4% paraformaldehyde in phosphate buffer (0.1 M, pH 7.4) for 1 hour at room temperature after 14 DIV. They were washed in PBS, incubated 1 hour in PBS 0.25% Triton-X-100 (PBST), 0.1 M gelatin (PBSTG) and 0.1% sodium azide, and then incubated with primary antibodies in PBSTG overnight at room temperature. After washing in PBST, slices were incubated with secondary antibodies in PBSTG for 2 hours at room temperature, washed in PBST and mounted in Mowiol.

Semi-automated image analysis of Purkinje cells

Photomicrographs of isolated Purkinje cells were acquired (Leica widefield DM6000 microscope, 40x oil objective) and the conditions (experimental procedure, transduced or not transduced) were recorded for each Purkinje cell in a file. Then, a blinded study to the experimental procedures was performed to categorise and analyse the dendritic tree of Purkinje cells using the ImagePro software. For each Purkinje cell, the following variables were measured: size of the soma, number of branch points in the dendritic arbour and length of the longest dendrite connecting to a given cell body. An algorithm was proposed to classify the different types of dendritic tree of Purkinje cells into 3 groups: atrophic, when the size of the longest dendrite was inferior to the soma diameter; stellate, when more than 6 primary dendrites of about the same size emerged from the cell body; and elaborate, including all the other ones. Among the Purkinje cells presenting an elaborate dendritic tree, we distinguished two types of Purkinje cells: the ones with spines, i.e presenting at least one part of their dendritic tree covered with spines, and the other ones that we called with no spines. On these elaborate Purkinje cells, a Sholl analysis was performed to estimate the distribution and complexity of the dendrites (Gutierrez and Davies, 2007). The Sholl analysis consisted of: (i) construction of concentric and equidistantly (10 µm) organized spherical shells centered at the cell body, (ii) counting the number of intersections of dendrites with the circles of increasing radii. To quantify dendritic length, branch points and Sholl analysis, Perl scripts were developed for parsing intermediate outputs.

Primary cell culture and transfection of hippocampal neurons

Neuronal hippocampal cultures were prepared from E17.5 day embryonic C57BL/6 mice and grown in Neurobasal medium supplemented with B27 and 10% Fetal bovine serum (FBS) (Raynaud et al., 2013). Neurons were transfected at DIV 8 with pSuper plasmids expressing the described shRNA sequences or plasmid DNA constructs of DOCK10, PAK3 or N-WASP and fixed at 11 DIV.

Subcellular fractionation

Synaptosomal fractions were prepared as follows: brains from euthanized P27 mice were placed in Hepes Buffer (20 mM Hepes pH 7.4, 0.32 M sucrose, EDTA 1 mM), subjected to dounce homogenization and subsequently centrifuged at 1'500*g* for 5 min, to remove nuclei and cell debris. The supernatant was centrifuged at 100'000*g* for 10 min. The resulting supernatant was saved (fraction S1: cytoplasmic fraction) and the pellet was resuspended in Hepes Buffer. This homogenate was carefully layered on top of a 0.85 M Sucrose Buffer and centrifuged at 9'000 *g* for 25 min. The resulting upper phase P1 (small vesicles) and middle phase P2 (synaptosomes) were collected and subjected to centrifugation at 100'000*g* for 10 min, while the pellet fraction P3 (membranes) was solubilized in Lysis Buffer (20 mM Hepes pH7.4, 100 mM NaCl, 2 mM EDTA, 1% Triton). The pellets resulting from the centrifuged P1 and P2 fractions were also solubilised in Lysis Buffer.

Immunofluorescence microscopy

Hippocampal neurons were fixed and permeabilized as previously described (Raynaud et al., 2013). Untreated or shRNA-GFP-expressing neurons were visualized using a Zeiss axio-imager Z1 microscope. For brain slices, we used a Zeiss LMS780 confocal microscope with a 63X 1.4 N.A. oil objective or a Leica widefield DM6000 microscope with a 100X 1.4 N.A. oil objective. Images were recorded with a CDD HQ2 devices camera (Roper scientific) controlled by Metamorph 7.1 (Universal Imaging).

Morphometric analyses were performed in different fields from at least three different cultures using the ImageJ software (National Institutes of Health, Bethesda, MD). Spines were defined as dendritic protrusions with a neck and a head. Dendrites were randomly selected, and spines manually counted over 50 µm length of dendrite. Data were then expressed as density of spines per 10 µm length of dendrite. The same spines were used to measure the area of their head. Each spine was manually traced and the surface calculated using the ImageJ software. All experiments were conducted in a double-blinded manner and dendritic spines were analysed from at least 20 neurons from at least three independent cultures (n=3 or 4 experiments, as indicated).

In vitro GEF assays

Fluorescence-based *in vitro* guanine-nucleotide exchange assays were performed using Mant-GTP (Molecular Probes) in an FLX 800 microplate fluorescence reader (BioTek Instruments) at 25°C, as described (Bouquier et al., 2009). Nucleotide exchange was determined by measuring Mant-GTP loading on GDP-preloaded Rac1, Cdc42 or RhoA GTPases using 1 µM GEF (0.5 µM for Dbl). The relative Mant fluorescence (λex = 360 nm and λem = 460 nm) was monitored for 30 min, and measurements were taken every 15 s.

Active GTPase pull-down

For the Rac1-GTP GST-pull-down assay, the CRIB domain of PAK was chosen, as described previously

(Briancon-Marjollet et al., 2008), while for Cdc42 the CRIB domain of N-WASP was used. Total HEK293T lysates and corresponding pull-downs retained on GST-Sepharose beads were processed for Western immunoblotting. RhoA-GTP pulldown assays were performed similarly, using the RBD domain of Rhotekin (Bouquier et al., 2009).

Statistical analysis

The distribution of Purkinje cell types was compared using the Pearson Chi2 test or Fisher's exact test depending on the amount. The Kruskal-Wallis test (non-parametric ANOVA) was used to compare Sholl index. All analyses were performed using the Statistical Package for the Social Sciences – SPSS version 20.0. Significance values were set at $p<0.05$.

SUPPLEMENTAL INFORMATION

Table S1: List of primers used in the Real-Time-quantitative PCR studies

Figure S1: Characterization of the shRNAs targeting DOCK10

Figure S2: Validation of the GEF-dead and the shRNA-resistant mutants of DOCK10

Figure S3: DOCK10 is not a GEF for RhoA

Figure S4: Schematic representation of the N-WASP and PAK3 constructs used in this study

ACKNOWLEDGEMENTS

We are grateful to Jean-Vianney Barnier (CNRS, UMR 8145, Paris) for the gift of PAK3 wt and kinase dead mutant constructs, to Michael Way (Cancer Research UK, London Research Institute) for the N-WASP mutant constructs and to Nathalie Morin for the N-WASP wt and WA constructs.

We thank Sylvie Fromont for assistance with molecular biology techniques, Jean-Michel Cioni for help with mouse perfusion techniques and Solange Desagher for introduction to RT-qPCR. The Montpellier Rio Imaging Facility, and in particular Virginie Georget, Sylvain de Rossi and Myriam Boyer-Clavel, are acknowledged for invaluable assistance with microscopy and FACS techniques. We are grateful to the Montpellier and Paris Mouse Housing facilities for animal care and maintenance. Finally we thank all members of the Debant lab and Gilles Gadea for helpful discussions and reading of the manuscript. The present work was supported by FUI RHENEPI and FUI DIATRAL grants (FR and LF) and ANR grant 07-Neuro-006-01 (AD).

REFERENCES

Ba, W., van der Raadt, J. and Nadif Kasri, N. (2013). Rho GTPase signaling at the synapse: implications for intellectual disability. *Exp Cell Res* 319, 2368-74.

Boukhtouche, F., Janmaat, S., Vodjdani, G., Gautheron, V., Mallet, J., Dusart, I. and Mariani, J. (2006). Retinoid-related orphan receptor alpha controls the early steps of Purkinje cell dendritic differentiation. *J Neurosci* 26, 1531-8.

Bouquier, N., Fromont, S., Zeeh, J. C., Auziol, C., Larrousse, P., Robert, B., Zeghouf, M., Cherfils, J., Debant, A. and Schmidt, S. (2009). Aptamer-derived peptides as potent inhibitors of the oncogenic RhoGEF Tgat. *Chem Biol* 16, 391-400.

Briancon-Marjollet, A., Ghogha, A., Nawabi, H., Triki, I., Auziol, C., Fromont, S., Piche, C., Enslen, H., Chebli, K., Cloutier, J. F. et al. (2008). Trio mediates netrin-1-induced Rac1 activation in axon outgrowth and guidance. *Mol Cell Biol* 28, 2314-23.

Cote, J. F., Motoyama, A. B., Bush, J. A. and Vuori, K. (2005). A novel and evolutionarily conserved PtdIns(3,4,5)P3-binding domain is necessary for DOCK180 signalling. *Nat Cell Biol* 7, 797-807.

Cote, J. F. and Vuori, K. (2002). Identification of an evolutionarily conserved superfamily of DOCK180-related proteins with guanine nucleotide exchange activity. *J Cell Sci* 115, 4901-13.

Cote, J. F. and Vuori, K. (2006). In vitro guanine nucleotide exchange activity of DHR-2/DOCKER/CZH2 domains. *Methods Enzymol* 406, 41-57.

Cote, J. F. and Vuori, K. (2007). GEF what? Dock180 and related proteins help Rac to polarize cells in new ways. *Trends Cell Biol* 17, 383-93.

Etienne-Manneville, S. and Hall, A. (2002). Rho GTPases in cell biology. *Nature* 420, 629-35.

Gadea, G., Sanz-Moreno, V., Self, A., Godi, A. and Marshall, C. J. (2008). DOCK10-mediated Cdc42 activation is necessary for amoeboid invasion of melanoma cells. *Curr Biol* 18, 1456-65.

Govek, E. E., Newey, S. E. and Van Aelst, L. (2005). The role of the Rho GTPases in neuronal development. *Genes Dev* 19, 1-49.

Gutierrez, H. and Davies, A. M. (2007). A fast and accurate procedure for deriving the Sholl profile in quantitative studies of neuronal morphology. *J Neurosci Methods* 163, 24-30.

Kasri, N. N. and van Aelst, L. (2008). Rho-linked genes and neurological disorders. *Pflugers Arch - Eur J Physiol* 455, 787-797.

Kim, J. Y., Oh, M. H., Bernard, L. P., Macara, I. G. and Zhang, H. (2011). The RhoG/ELMO1/Dock180 signaling module is required for spine morphogenesis in hippocampal neurons. *J Biol Chem* 286, 37615-24.

Kiraly, D. D., Eipper-Mains, J. E., Mains, R. E. and Eipper, B. A. (2010). Synaptic plasticity, a symphony in GEF. *ACS Chem Neurosci* 1, 348-365.

Kreis, P., Thevenot, E., Rousseau, V., Boda, B., Muller, D. and Barnier, J. V. (2007). The p21-activated kinase 3 implicated in mental retardation regulates spine morphogenesis through a Cdc42-dependent pathway. *J Biol Chem* 282, 21497-506.

Kulkarni, K., Yang, J., Zhang, Z. and Barford, D. (2011). Multiple factors confer specific Cdc42 and Rac protein activation by dedicator of cytokinesis (DOCK) nucleotide exchange factors. *J Biol Chem* 286, 25341-51.

Kuramoto, K., Negishi, M. and Katoh, H. (2009). Regulation of dendrite growth by the Cdc42 activator Zizimin1/Dock9 in hippocampal neurons. *J Neurosci Res* 87, 1794-805.

Lebrun, C., Avci, H. X., Wehrle, R., Doulazmi, M., Jaudon, F., Morel, M. P., Rivals, I., Ema, M., Schmidt, S., Sotelo, C. et al. (2013). Klf9 is necessary and sufficient for Purkinje cell survival in organotypic culture. *Mol Cell Neurosci* 54, 9-21.

Lin, Q., Yang, W., Baird, D., Feng, Q. and Cerione, R. A. (2006). Identification of a DOCK180-related guanine nucleotide exchange factor that is capable of mediating a positive feedback activation of Cdc42. *J Biol Chem* 281, 35253-62.

Lu, M., Kinchen, J. M., Rossman, K. L., Grimsley, C., Hall, M., Sondek, J., Hengartner, M. O., Yajnik, V. and Ravichandran, K. S. (2005). A Steric-inhibition model for regulation of nucleotide exchange via the Dock180 family of GEFs. *Curr Biol* 15, 371-7.

Lutfalla, G. and Uze, G. (2006). Performing quantitative reverse-transcribed polymerase chain reaction experiments. . *Methods in enzymology* 410, 386-400.

Momboisse, F., Lonchamp, E., Calco, V., Ceridono, M., Vitale, N., Bader, M. F. and Gasman, S. (2009). betaPIX-activated Rac1 stimulates the activation of phospholipase D, which is associated with exocytosis in neuroendocrine cells. *J Cell Sci* 122, 798-806.

Nava, C., Keren, B., Mignot, C., Rastetter, A., Chantot-Bastaraud, S., Faudet, A., Fonteneau, E., Amiet, C., Laurent, C., Jacquette, A. et al. (2013). Prospective diagnostic analysis of copy number variants using SNP microarrays in individuals with autism spectrum disorders. *Eur J Hum Genet*.

Newey, S. E., Velamoor, V., Govek, E. E. and Van Aelst, L. (2005). Rho GTPases, dendritic structure, and mental retardation. *J Neurobiol* 64, 58-74.

Nishikimi, A., Meller, N., Uekawa, N., Isobe, K., Schwartz, M. A. and Maruyama, M. (2005). Zizimin2: a novel, DOCK180-related Cdc42 guanine nucleotide exchange factor expressed predominantly in lymphocytes. *FEBS Lett* 579, 1039-46.

Pakes, N. K., Veltman, D. M. and Williams, R. S. (2013). Zizimin and Dock guanine nucleotide exchange factors in cell function and disease. *Small GTPases* 4, 22-7.

Penzes, P., Beeser, A., Chernoff, J., Schiller, M. R., Eipper, B. A., Mains, R. E. and Huganir, R. L. (2003). Rapid induction of dendritic spine morphogenesis by trans-synaptic ephrinB-EphB receptor activation of the Rho-GEF kalirin. *Neuron* 37, 263-74.

Poulain, F. E., Chauvin, S., Wehrle, R., Desclaux, M., Mallet, J., Vodjdani, G., Dusart, I. and Sobel, A. (2008). SCLIP is crucial for the formation and development of the Purkinje cell dendritic arbor. *J Neurosci* 28, 7387-98.

Raynaud, F., Janossy, A., Dahl, J., Bertaso, F., Perroy, J., Varrault, A., Vidal, M., Worley, P. F., Boeckers, T. M., Bockaert, J. et al. (2013). Shank3-Rich2 Interaction Regulates AMPA Receptor Recycling and Synaptic Long-term Potentiation. *J Neurosci* in press.

Rohatgi, R., Ma, L., Miki, H., Lopez, M., Kirchhausen, T., Takenawa, T. and Kirschner, M. W. (1999). The interaction between N-WASP and the Arp2/3 complex links Cdc42-dependent signals to actin assembly. *Cell* 97, 221-31.

Santamaria, J., Khalfallah, O., Sauty, C., Brunet, I., Sibieude, M., Mallet, J., Berrard, S. and Lecomte, M. J. (2009). Silencing of choline acetyltransferase expression by lentivirus-mediated RNA interference in cultured cells and in the adult rodent brain. *J Neurosci Res* 87, 532-44.

Schmidt, A. and Hall, A. (2002). Guanine nucleotide exchange factors for Rho GTPases: turning on the switch. *Genes Dev* 16, 1587-609.

Sotelo, C. and Dusart, I. (2009). Intrinsic versus extrinsic determinants during the development of Purkinje cell dendrites. *Neuroscience* 162, 589-600.

Tada, T. and Sheng, M. (2006). Molecular mechanisms of dendritic spine morphogenesis. *Curr Opin Neurobiol* 16, 95-101.

Tanaka, M. (2009). Dendrite formation of cerebellar Purkinje cells. *Neurochem Res* 34, 2078-88.

Tolias, K. F., Bikoff, J. B., Burette, A., Paradis, S., Harrar, D., Tavazoie, S., Weinberg, R. J. and Greenberg, M. E. (2005). The Rac1-GEF Tiam1 couples the NMDA receptor to the activity-dependent development of dendritic arbors and spines. *Neuron* 45, 525-38.

Tolias, K. F., Bikoff, J. B., Kane, C. G., Tolias, C. S., Hu, L. and Greenberg, M. E. (2007). The Rac1 guanine nucleotide exchange factor Tiam1 mediates EphB receptor-dependent dendritic spine development. *Proc Natl Acad Sci U S A* 104, 7265-70.

Tolias, K. F., Duman, J. G. and Um, K. (2011). Control of synapse development and plasticity by Rho GTPase regulatory proteins. *Prog Neurobiol* 94, 133-48.

Tomomura, M., Rice, D. S., Morgan, J. I. and Yuzaki, M. (2001). Purification of Purkinje cells by fluorescence-activated cell sorting from transgenic mice that express green fluorescent protein. *Eur J Neurosci* 14, 57-63.

Ueda, S., Negishi, M. and Katoh, H. (2013). Rac GEF Dock4 interacts with cortactin to regulate dendritic spine formation. *Mol Biol Cell* 24, 1602-13.

Urbanska, M., Blazejczyk, M. and Jaworski, J. (2008). Molecular basis of dendritic arborization. *Acta Neurobiol Exp (Wars)* 68, 264-88.

Vadodaria, K. C., Brakebusch, C., Suter, U. and Jessberger, S. (2013). Stage-specific functions of the small Rho GTPases Cdc42 and Rac1 for adult hippocampal neurogenesis. *J Neurosci* 33, 1179-89.

Vandesompele, J., De Preter, K., Pattyn, F., Poppe, B., Van Roy, N., De Paepe, A. and Speleman, F. (2002). Accurate normalization of real-time quantitative RT-PCR data by geometric averaging of multiple internal control genes. *Genome Biology* 3, 0034.1-0034.11.

Wegner, A. M., Nebhan, C. A., Hu, L., Majumdar, D., Meier, K. M., Weaver, A. M. and Webb, D. J. (2008). N-wasp and the arp2/3 complex are critical regulators of actin in the development of dendritic spines and synapses. *J Biol Chem* 283, 15912-20.

Yang, J., Zhang, Z., Roe, S. M., Marshall, C. J. and Barford, D. (2009). Activation of Rho GTPases by DOCK exchange factors is mediated by a nucleotide sensor. *Science* 325, 1398-402.

Yuste, R. and Bonhoeffer, T. (2004). Genesis of dendritic spines: insights from ultrastructural and imaging studies. *Nat Rev Neurosci* 5, 24-34.

Zennou, V., Serguera, C., Sarkis, C., Colin, P., Perret, E., Mallet, J. and Charneau, P. (2001). The HIV-1 DNA flap stimulates HIV vector-mediated cell transduction in the brain. *Nat Biotechnol* 19, 446-50.

Zufferey, R., Nagy, D., Mandel, R. J., Naldini, L. and Trono, D. (1997). Multiply attenuated lentiviral vector achieves efficient gene delivery in vivo. *Nat Biotechnol* 15, 871-5.

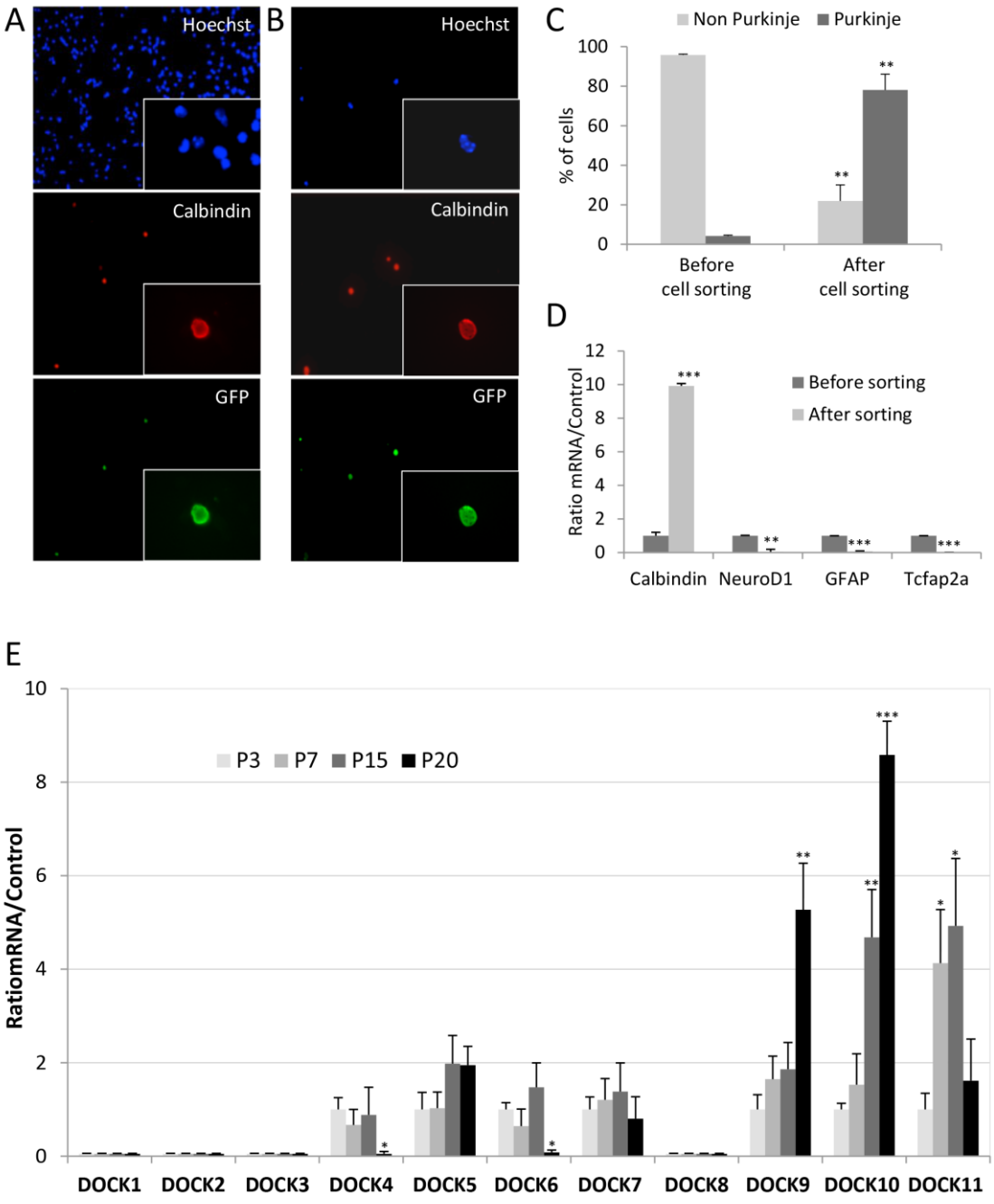

Jaudon et al, Figure 1

Figure 1: Gene expression profiling of all DOCK RhoGEFs in purified postnatal Purkinje neurons.

(A and B) Sorting of GFP-expressing postnatal Purkinje neurons by FACS. Dissociated cells from cerebella of Pcp2-GFP mice at P3, P7, P15 and P20 were plated before (A) and after (B) sorting, and fixed. Nuclei were stained with Hoechst to visualise the total cell number in the sample, and Purkinje neurons were revealed with a Calbindin antibody (red) and by direct fluorescence of the GFP (green). Micrographs show representative sorting results of cerebellar cells from mice at P7.

(C) Histogram representing the enrichment of Purkinje neurons within the cell population upon sorting, expressed as relative percentages. Data are expressed as the mean enrichment value of all age groups combined ± the standard deviation of at least 3 independent experiments. **p<0.01 (Student's t test).

(D) Quantitative RT-qPCR performed before and after FACS on the mRNA of specific marker genes of the main cerebellar cell types, Calbindin (Purkinje cells), NeuroD1 (cerebellar granule neurons), GFAP (astrocytes) and Tcfap2a (interneurons). Data are expressed as the mean ± standard deviation of at least 3 experiments, performed on postnatal stage P7 Pcp2-GFP mice in the example shown. **p<0.01 and ***p<0.001 (Student's t test).

(E) Quantitative RT-qPCR performed on purified PC mRNAs of all 11 mammalian DOCK family RhoGEFs. Data are expressed as the mean ± standard deviation of at least 3 experiments. *p<0.05, **p<0.01 and ***p<0.001 (Student's t test).

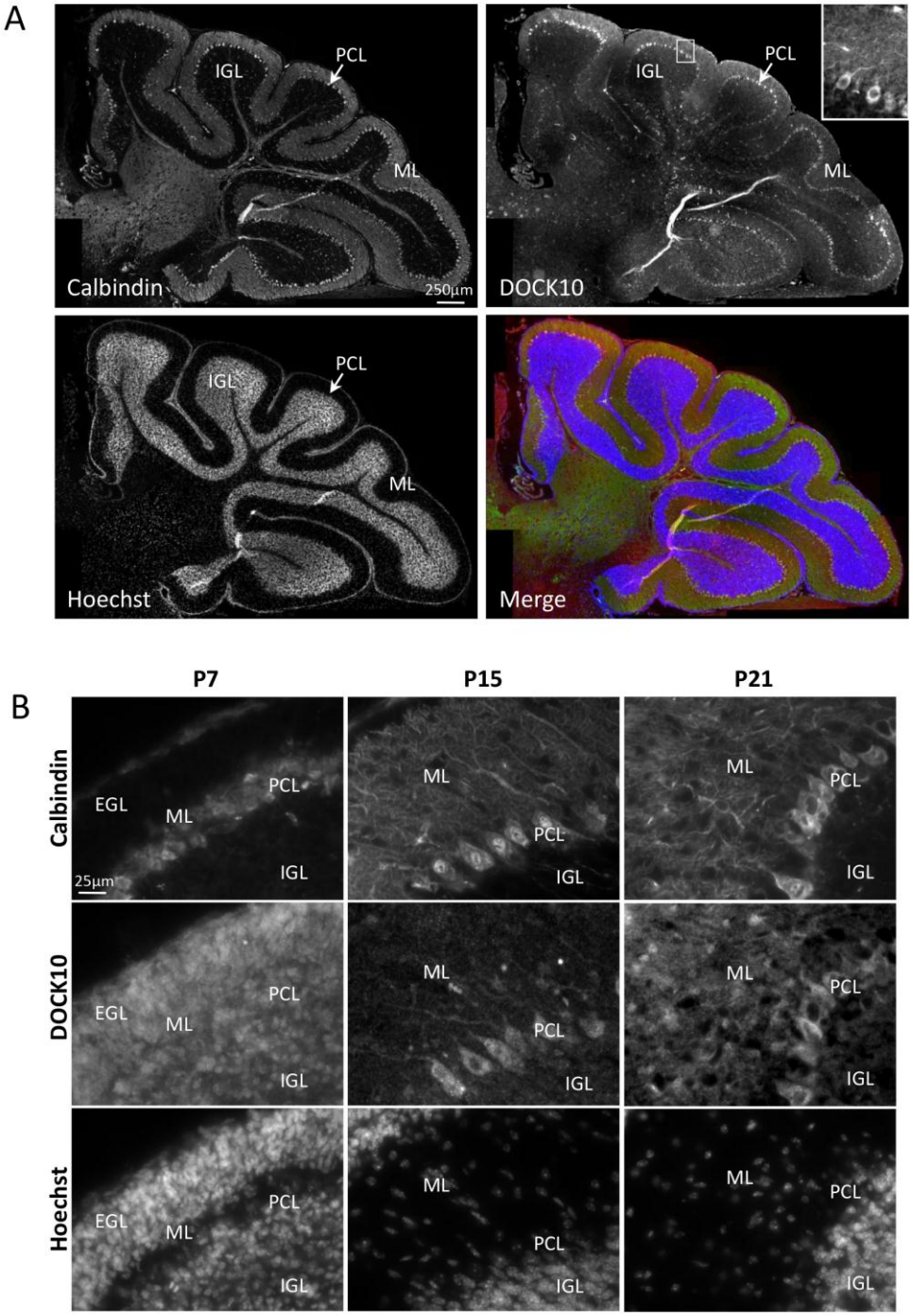

Jaudon et al, Figure 2

Figure 2: DOCK10 expression in cerebellar Purkinje cells at postnatal stages.

(A) Immunohistochemistry performed on wild type C57BL/6 mouse cerebellar sections at P15, using a DOCK10 antibody (red) and a Calbindin antibody to label the PCs (green). Nuclei were stained with Hoechst (blue) to visualise all cells in the slice. Due to the high density of granule cells, the latter staining highlights mainly the IGL. A merged image is shown at the bottom right of the figure. Note the monolayer-specific staining of PCs, revealed with both the DOCK10 antibody and the Calbindin antibody. These antibodies also label the Purkinje cell dendritic tree in the molecular layer. The inset is a higher magnification image of the boxed region, to show the DOCK10 immunostaining. IGL: Internal Granule cell Layer; PCL: Purkinje Cell Layer; ML: Molecular Layer. Scale bar: 250 µm.

(B) Immunohistochemistry performed on P7, P15 and P21 C57BL/6 mouse brain sections, using a DOCK10 and a Calbindin antibody. Nuclei were stained with Hoechst to visualise all cells in the slice. The various cell layers found in the section are indicated as in (A); EGL: External Granule cell Layer. Note the Purkinje cell-specific staining of DOCK10 at P15 and P21 in the soma and to a lesser extent in the dendritic tree (see also inset in A). Scale bar: 25 µm.

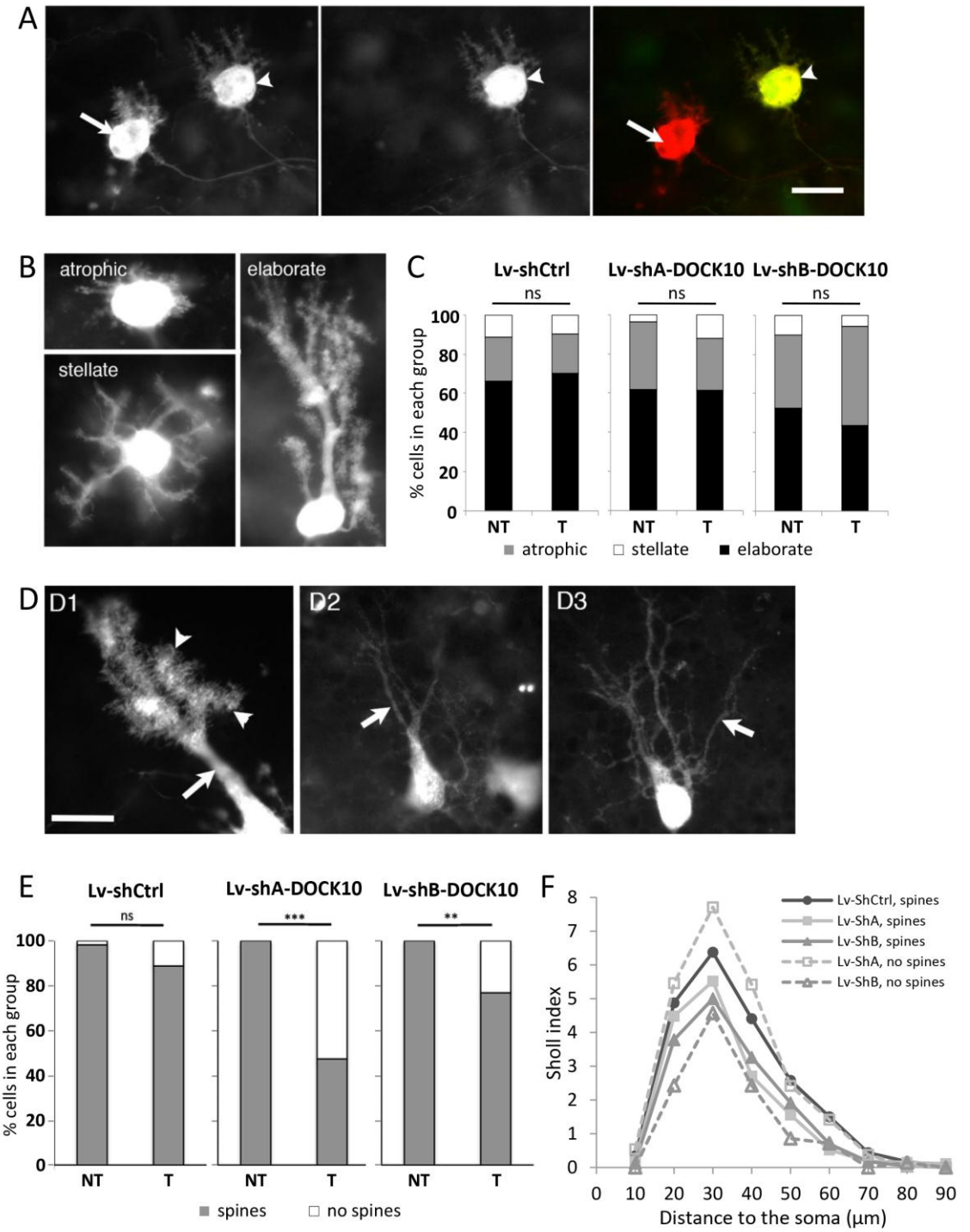

Jaudon et al, Figure 3

Figure 3: Depletion of DOCK10 in Purkinje cells leads to dendritic spine defects

(A) Micrographs of organotypic cultures that received Lv-ShA DOCK10. The arrowhead represents a transduced Purkinje cell (GFP+/Calbindin+) whereas the arrow represents a non transduced Purkinje cell (GFP-/Calbindin+). Scale bar: 18.75µm.

(B) Micrographs illustrating typical Calbindin labelled PCs observed in organotypic cultures after 14 DIV: atrophic, stellate, and elaborate PCs.

(C) Histograms representing the distribution of Purkinje cell types 14 DIV after transduction with lentiviral vectors expressing the GFP marker together with either a control shRNA or the two DOCK10 shRNAs shA and shB. Data are presented as relative percentage for each stage in non transduced (NT) and transduced (T) PCs. For statistical analysis, the distributions of Purkinje cell types were compared using the Pearson Chi2 test or Fisher's exact test depending on the amount of PCs per group (non-significant differences were detected, $p>0.5$).

(D) Micrographs of Calbindin-labelled Purkinje cells within organotypic cultures after 14 DIV and lentiviral infection. (D1) is a non-transduced Purkinje cell, whereas (D2) and (D3) is a Purkinje cell transduced with shA DOCK10 and shB DOCK10, respectively. Arrowheads point to a dendritic area covered with spines, arrow to a naked dendritic area (devoid of spines). Scale bar: 18.75 µm.

(E) Histograms representing the distribution of Purkinje cells distinguishing cells with at least one part of the dendritic tree covered with spines (spines) and cells with a dendritic tree devoid of spines (no spines) following transduction by lentiviral vectors as described in (C). Data are presented as relative percentage for each group. Compared are non-transduced Purkinje cells (NT) and transduced PCs (T). For statistical analysis, the distributions of Purkinje cell types were compared using the Pearson Chi2 test or Fisher's exact test depending on the amount of PCs per group (ns non-significant, ** $p<0.005$, *** $p<0.001$).

(F) Sholl analysis of PCs with an elaborate dendritic tree in the different experimental groups. Sholl analysis was performed on cells with at least one part of the dendritic tree covered with spines (spines) and cells with a dendritic tree devoid of spines (no spines) in the different transduced conditions (shCtlr, shA DOCK10, and shB DOCK10).

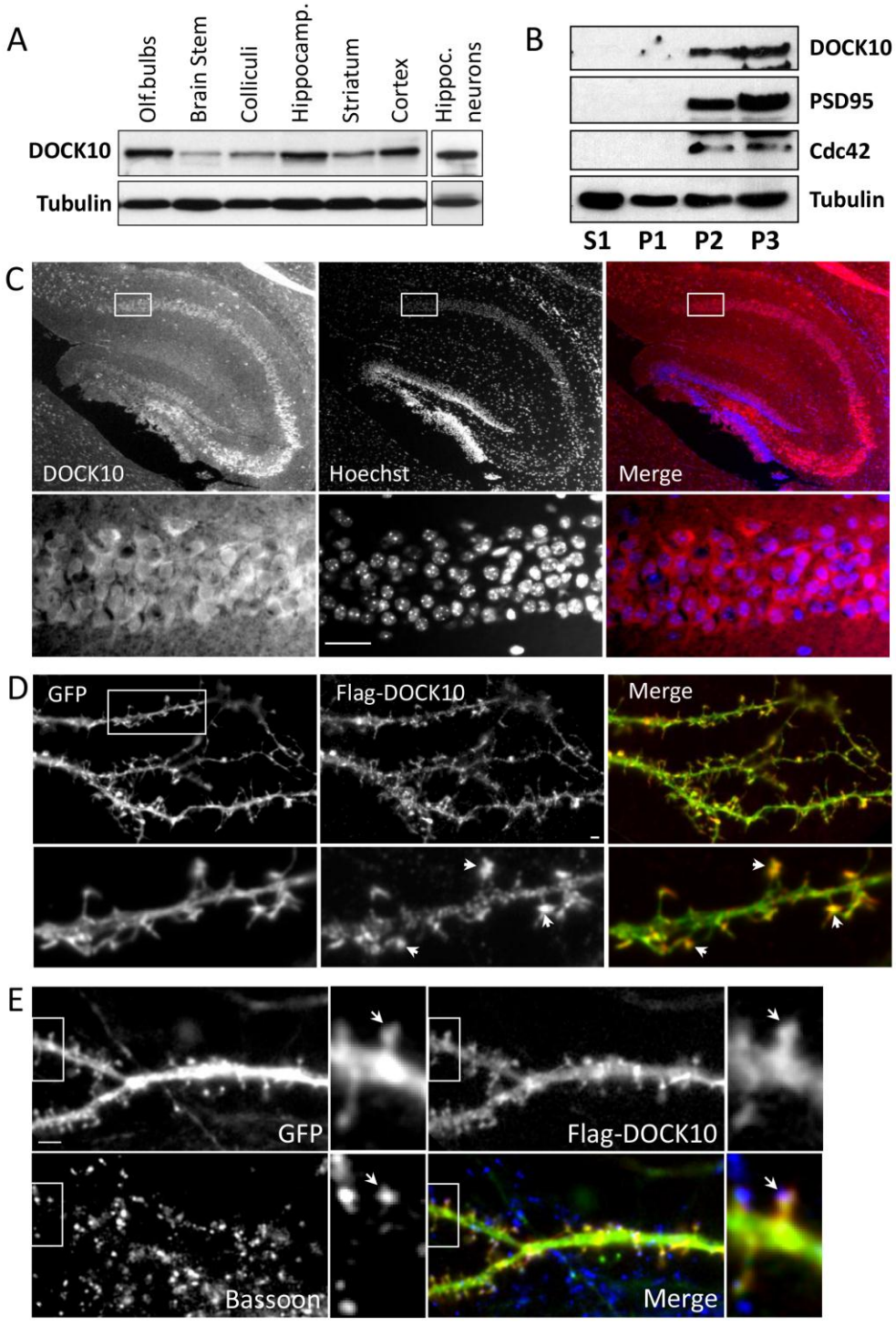

Jaudon et al, Figure 4

Figure 4: DOCK10 is expressed in the hippocampus and localised in dendritic spines in hippocampal neurons

(A) Protein extracts from various P26 mouse brain regions and from cultured hippocampal neurons at 18 DIV were analysed by Western blot, using a DOCK10 antibody. Tubulin was used as a loading control.

(B) Subcellular fractions, obtained after fractionation of P27 mouse brain extracts on a sucrose gradient, were analysed by Western blot, using a DOCK10, a PSD-95 and a Cdc42 antibody. Tubulin was used as a loading control. S1: soluble cytoplasmic fraction; P1, vesicular fraction; P2, synaptosomal fraction; P3, membrane fraction.

(C) Immunohistochemistry performed on stage P15 mouse hippocampus sections. Immunostaining was performed using a DOCK10 antibody (red). Nuclei were stained with Hoechst (blue) to visualise all cells in the slice. Due to the high density of cells, the latter staining highlights mainly the dentate gyrus. A merged image is shown in the right hand panels of the figure. Panels underneath each image are higher magnification images of the region selected in the above panels (CA1/Subiculum region). Scale bar: 40 μm.

(D) DOCK10 is localised in dendrites and spines of hippocampal neurons. Shown are micrographs of cultured hippocampal neurons co-transfected with flag-DOCK10 (detected with an anti-flag antibody; red) and GFP, to visualise the dendrites (green). Merged images are shown on the right. Lower panels are higher magnification images of the region selected in the upper panels. Scale bar: 1μm. Arrows: examples of spine heads labelled by DOCK10.

(E) DOCK10 post-synaptic localisation is adjacent to pre-synaptic terminals. Shown are micrographs of hippocampal neurons co-transfected with flag-DOCK10 (detected with an anti-flag antibody; red; top right panel) and GFP, to visualise the dendrites (green; top left panel). Immunostaining was performed using an anti-Bassoon antibody (blue, bottom left panel), which marks the pre-synaptic terminals. A merged image is shown in the bottom right panel of the figure. The insets are higher magnification images of a selected region, to better visualize the adjacent localisation of DOCK10 and Bassoon (arrows).

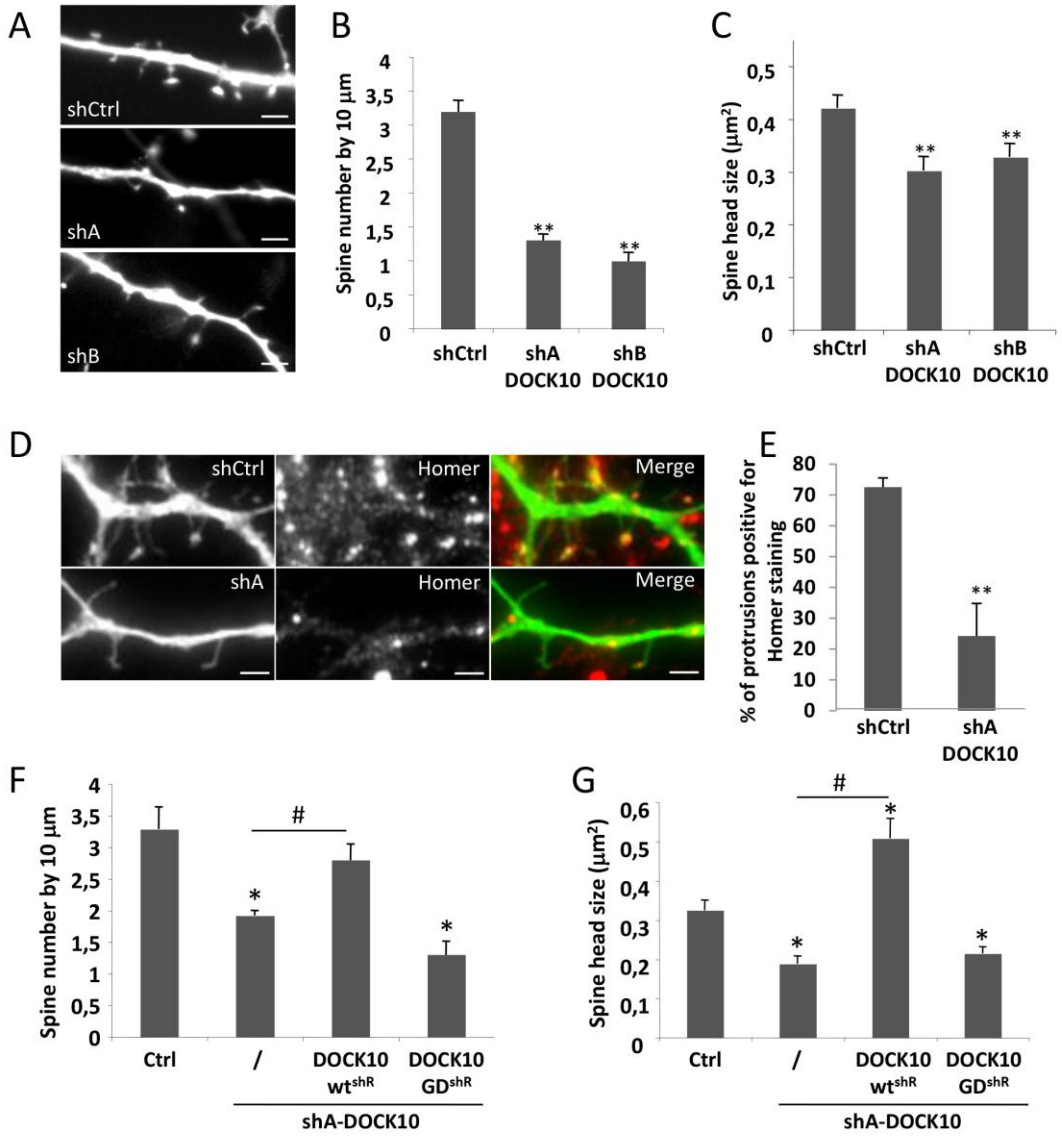

Jaudon et al, Figure 5

Figure 5: The GEF activity of DOCK10 is required for the formation of dendritic spines in hippocampal neurons

(A) Depletion of DOCK10 leads to decreased spine density and spine head size. Shown are representative micrographs of hippocampal neurons transfected with a control shRNA (shCtrl) or two different DOCK10 shRNAs (shA and shB). Neurons were transfected at 8 DIV and fixed at 11 DIV (experimental conditions to reveal spine formation). Scale bar: 1 µm.

(B and C) Quantification of dendritic spine density (B) and size (C) of hippocampal neurons transfected as described in (A), measured by the number of spines/10 µm and the spine head area, respectively. Error bars indicate the SEM (n=3 independent experiments), **p<0.01 (Student's t-test).

(D) Shown are representative micrographs of hippocampal neurons transfected with shA DOCK10 or shCtrl (green) and immunostained for post-synaptic protein Homer-1 (red; middle micrographs). Merged images are shown on the right. Scale bar: 1 µm.

(E) Quantification of the number of protrusions positive for Homer-1 staining in DOCK10-depleted or control neurons, as described in (D). Error bars indicate the SEM (n=4 independent experiments), **p=0.001 (Student's t-test).

(F and G) A functional GEF activity of DOCK10 is required for spine formation in hippocampal neurons. Quantification of spine density (F) and size (G) of hippocampal neurons co-transfected with shA-DOCK10 and either a control vector or shA-resistant wt DOCK10^{shR} or shA-resistant GEF-dead DOCK10 (DOCK10 GD ^{shR}). Error bars indicate the SEM (n=3 independent experiments), * p< 0.05, # p< 0.05 (Student's t-test).

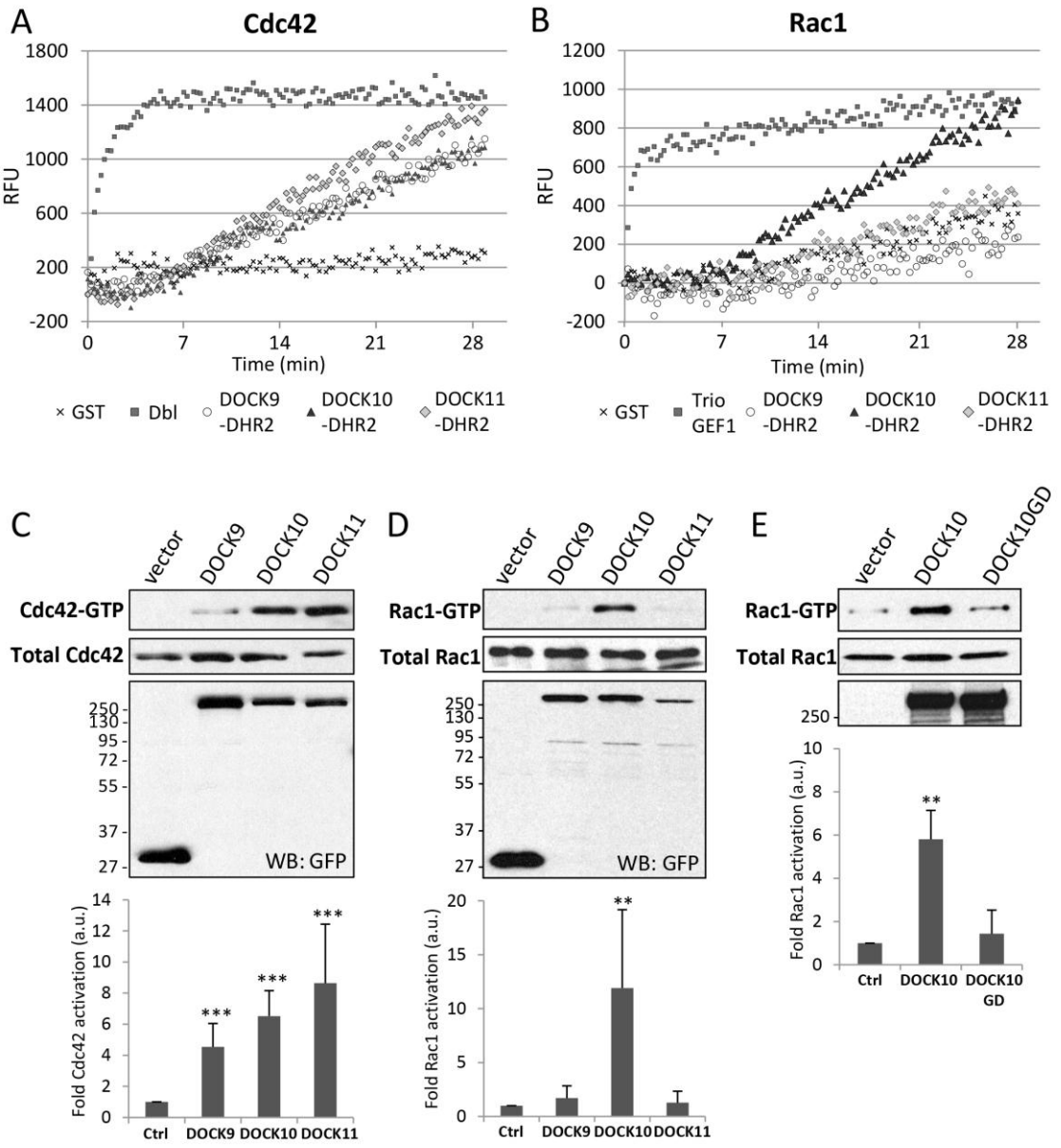

Jaudon et al, Figure 6

Figure 6: DOCK10 is a GEF for Rac1 and Cdc42 *in vitro* and in cells.

(A and B) *In vitro* GEF assay performed on Cdc42 (A) and Rac1 (B), using GST-DHR2-domains of DOCK9, DOCK10 and DOCK11. GST-Dbl and GST-Trio GEF1 were used as positive control GEFs for Cdc42 and Rac1, respectively, while GST alone was used as negative control. Results are expressed as relative fluorescence units (RFU) versus time.

(C, D and E) Active GTPase pull-down assays. GTP-loaded Cdc42 (C) or GTP-loaded Rac1 (D and E) were pulled down from protein lysates of HEK293 cells expressing either wild-type pEGFP-DOCK9, -10 or -11 constructs or DOCK10 GD. GFP vector was used as a negative control. Shown are representative experiments. GTP-bound and total Cdc42 or Rac1 were detected by Western blot, using anti-Cdc42 and anti-Rac1 antibodies, respectively. Protein expression in the cell lysates was verified by immunoblotting with an anti-GFP antibody.

Histograms underneath each Western blot show the quantification of the above corresponding GTPase activation assays. The ratio of GTP-Rac1 (or Cdc42) over total Rac1 (or Cdc42) was calculated from at least 3 independent experiments. Error bars indicate the SEM, ** $p< 0.003$, *** $p<0.0001$.

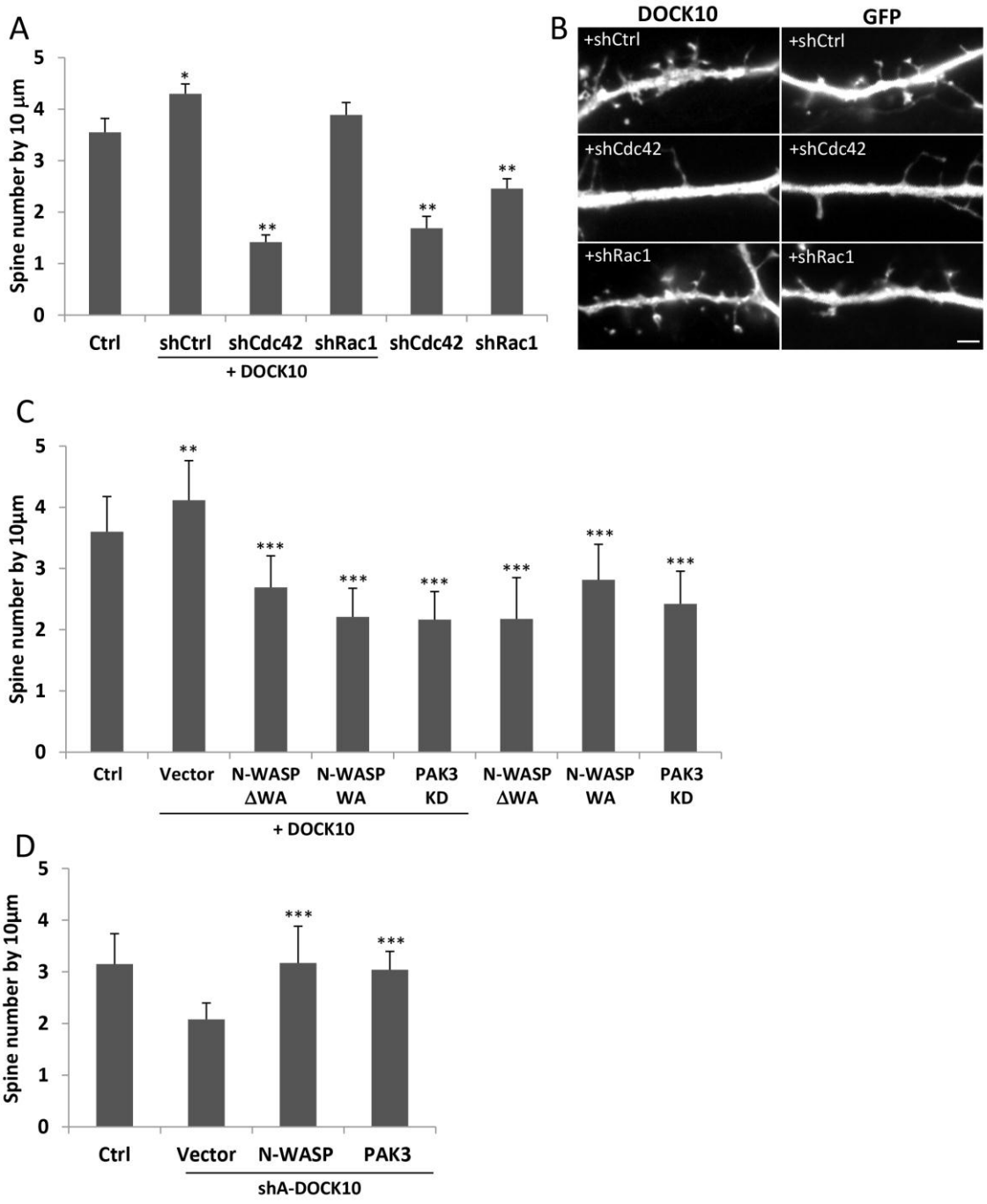

Jaudon et al, Figure 7

Figure 7: DOCK10 regulates spine formation via Cdc42-N-WASP and -PAK3 pathways

(A) The effects of DOCK10 on spine formation are mediated by Cdc42. Quantification of dendritic spine density, measured as described in Figure 5B, of hippocampal neurons transfected shRNAs alone targeting either Cdc42 or Rac1 (Momboisse et al., 2009) (or control shRNA), or in combination with DOCK10. Appropriate experimental conditions (transfection at 8 DIV and fixation at 11 DIV) were used to quantify formation of spines. Error bars indicate the SEM (n=3 independent experiments), **p<0.01 (p-value obtained by Student's t-test).)

(B) Shown are representative micrographs of hippocampal neurons transfected as described in A. Scale bar is indicated (1 µm).

(C) Quantification of dendritic spine density, measured as described in Figure 5B, of hippocampal neurons transfected with N-WASPΔWA, N-WASPWA, or PAK3KD alone or in combination with DOCK10. Appropriate experimental conditions as in A were used to quantify formation of spines. Error bars indicate the SEM (n=3 independent experiments), **p<0.01, ***p<0.001 (p-value obtained by Student's t-test).

(D) Quantification of dendritic spine density, measured as described in Figure 5B, of hippocampal neurons transfected with sh Ctrl or shA-DOCK10 in combination with N-WASP or PAK3. Appropriate experimental conditions as in A were used to quantify formation of spines. Error bars indicate the SEM (n=3 independent experiments), ***p<0.001 (p-value obtained by Student's t-test).